

## Estimation of excitation and reaction forces for offshore structures by neural networks

Ahmed A. Elshafey<sup>\*1</sup>, M.R. Haddara<sup>2a</sup> and H. Marzouk<sup>3b</sup>

<sup>1</sup>Faculty of Engineering, Minoufiya University and a PDF, Memorial University of Newfoundland, Canada

<sup>2</sup>Faculty of Engineering, Memorial University of Newfoundland, Canada

<sup>3</sup>Faculty of Engineering, Architecture and Science, Ryerson University, Toronto, Canada

(Received November 23, 2010, Accepted February 10, 2011)

**Abstract.** Offshore structures are subjected to wind loads, wind generated wave excitations, and current forces. In this paper we focus on the wind generated wave excitations as the main source for the external forces on the structure. The main objective of the paper is to provide a tool for using deck acceleration measurements to predict the value of the force and moment acting on the offshore structure foundation. A change in these values can be used as an indicator of the health of the foundation. Two methods of analysis are used to determine the relationship between the force and moment acting on the foundation and deck acceleration. The first approach uses neural networks while the other uses a Fokker-Planck formulation. The Fokker-Planck approach was used to relate the variance of the excitation to the variance of the deck acceleration. The total virtual mass of the equivalent SDOF of the structure was also determined at different deck masses.

**Keywords:** offshore platform, wave excitation, neural networks, Fokker-Planck equation, reaction force.

---

### 1. Introduction

Neural networks have been used successfully to predict the dynamic characteristics of offshore structures. Back propagation neural networks (BPNN) were used to estimate the unknown parameters of offshore structures (Yun and Bahng 1997). Banerji and Datta (1997) developed a technique using artificial neural networks (ANN) to monitor the structural integrity of offshore platforms. The feed-forward, back-propagation neural networks were used to assess the accumulated fatigue damage at joints of fixed offshore structures based on the measurements of upward jacket displacements (Lopes 1997; Lopes and Ebecken 1997). A back-propagation neural network model was developed to predict the uplift capacity of suction caissons using results from centrifuge tests (Rahman *et al.* 2001). Zubaydi *et al.* (2002) used a neural networks approach to detect the damage occurring on the side shell of a ship's hull. The complicated dynamic problem of turret-FPSO (Floating Production Storage and Off-loading) system was studied using neural networks based on real data measurements to avoid possible collisions and mooring line stress (Simões *et al.* 2002). Neural network algorithm was proposed to reconstruct wave height time series using a weighted error

---

\*Corresponding author, Assistant professor, E-mail: [aeshafey@mun.ca](mailto:aeshafey@mun.ca)

<sup>a</sup>Professor

<sup>b</sup>Chair and Professor

function during the learning phase to improve the modelling of higher significant wave heights (Arena and Puca 2004). Predictions of wave heights at five different locations around North America were done using ANN. The predicted waves were valid for durations of 6 to 12 hours depending on the location (Londhe and Panchang 2005). Diao *et al.* (2005) used ANN to localize the damage in offshore platforms. Budipriyanto *et al.* (2007) used a neural networks approach to detect damage in cross stiffened plates. An experimental study of wave forces on vertical cylinders in shallow waters was carried out in a wave channel and results were compared with different wave theories (Ma *et al.* 2007). Fathi and Aghakouchak (2007) used artificial neural networks to predict stress intensity modification factors for the deepest point of fatigue cracks and fatigue lives of tubular T-joints. Probabilistic neural network was used to control the response of offshore structures subjected to random ocean waves (Chang *et al.* 2009). A combination of the method of random decrement and neural networks was applied to detect the damage in offshore structures (Elshafey *et al.* 2010). A Fokker-Planck approach to estimate the dynamic parameters and excitation for ships and offshore structures was used by Haddara (2006) and Elshafey *et al.* (2009, 2010).

This paper provides a tool for estimating the values of the reaction force and bending moment at the foundation of an offshore platform using the deck acceleration measurements. The foundation health can be monitored using the values of the reaction forces and moment. The relationship between the deck acceleration and the force and moment at foundation was determined using two approaches; the first is the neural networks and the second is the Fokker-Plank formula. The experimental work was done on an offshore single column platform and can be extended to other fixed platforms.

## 2. The experimental model of a single offshore structure

A scaled model for a single column offshore structure is used in the experiments. The model is made of an acrylic pipe having a constant circular cross section. The pipe is attached rigidly at the bottom to a base while its top is free. The stress strain relationship for the model material can be considered linear in the area of interest. The external diameter of the cross section of the model is 2 1/2 inches and the internal diameter is 2 1/4 inches. A mass holder is attached to the free end of the model to allow additional masses to be attached to the free end of the model. The bottom end of the model was attached rigidly to a 3" thick acrylic base using Dichloromethane solvent material. The acrylic base was in turn attached to a 1/2" steel flat plate using a number of steel bolts. This arrangement ensures that the boundary condition at the bottom end of the model is considered fixed. Fig. 1 shows the general layout and dimensions of the model. The levels shown in Fig. 1 are in meters. Fig. 2 shows the model inside the wave tank ready for the experiment.

## 3. Testing the material of the model

The material of the model was tested under tension to determine its modulus of elasticity. Three specimens were prepared and tested. The stress strain relationships obtained for these specimens are shown in Fig. 3. The results obtained for the three specimens show a very close agreement. The material shows linear behavior up to a strain of 0.01. For strains greater than 0.01 the behavior becomes nonlinear. The experimental range lies within the linear part of the stress-strain curve. A

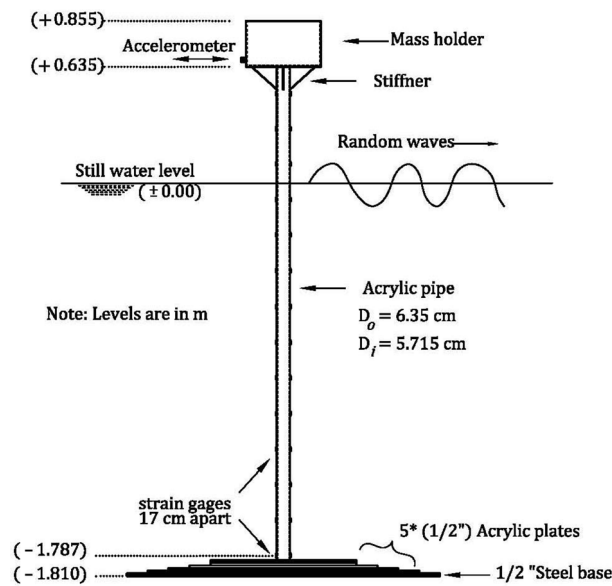


Fig. 1 General layout and dimensions of the model

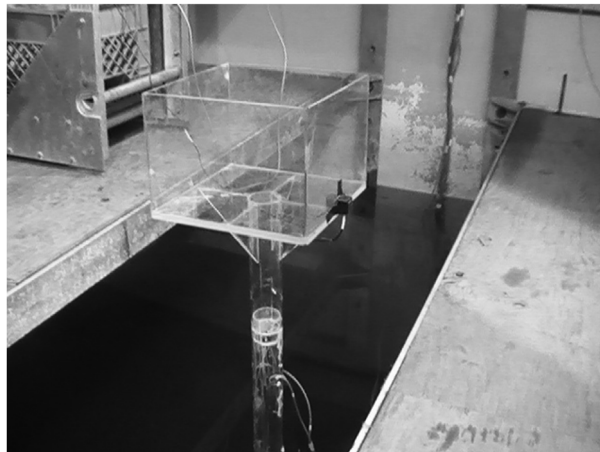


Fig. 2 The model in the wave tank

value of  $1.85 \times 10^9 \text{ N/m}^2$  was obtained for the modulus of elasticity for the material. The material density is  $1190 \text{ kg/m}^3$ . The material properties are used to estimate both the bending moment and reaction force at the base of the structure as discussed in coming sections.

#### 4. Experimental setup and model instrumentation

The model was instrumented by an accelerometer mounted on the mass holder as shown in Figs. 1, 2, and 4. Pairs of strain gages were attached along the length of the model at levels 17 cm apart. At each level, two strain gages were attached to model: one at the fore and the second at the aft of

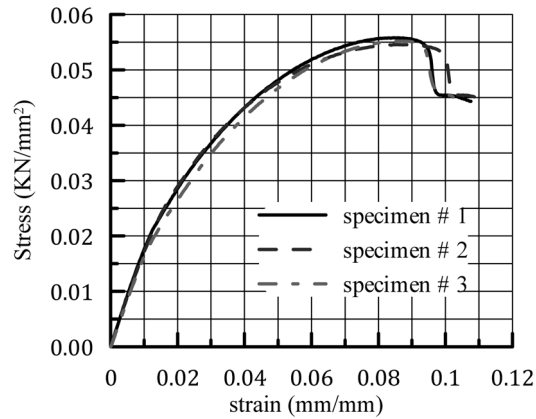


Fig. 3 Stress-strain relationship for the model material

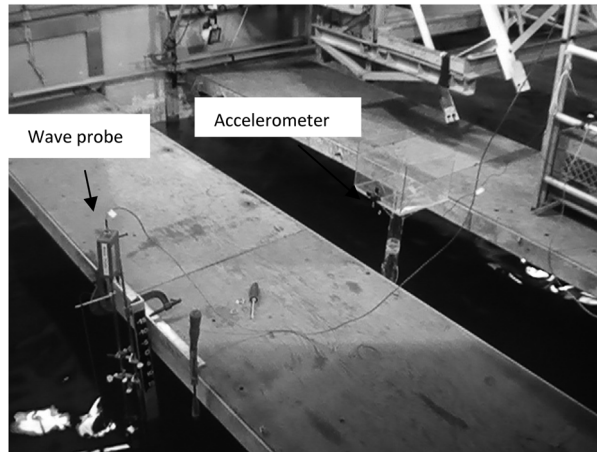


Fig. 4 The structure under test

the model. Several coats of an agent called NG 150 were applied to each strain gage. This guaranteed an excellent watertight protection for the strain gages. The model was tested in the towing tank using random waves. A wave probe was used to measure wave heights, see Fig. 4. All measuring devices were calibrated before the start of the experiment. The data was collected using Labview software and NI data acquisition system at a frequency of 100 Hz. A time history of 500 sec is recorded for each experiment.

## 5. Generation of irregular wave excitation

The model was tested in the wave tank of Memorial University. The towing tank is equipped at one end with a wave board that can generate both regular and irregular waves, and at the other end with a wave absorbing beach to minimize wave reflection. The model was tested using irregular waves in water of depth of 1.81 m. Random waves having a JONSWAP spectrum were used in the experiment. The spectrum is given by

$$S(f) = \frac{A}{f^5} e^{-\left(\frac{B}{f^4}\right)} \gamma^\alpha \quad (1)$$

where;

$$A = \frac{5H_s^2 f_o^4}{16\gamma^{1/3}} \quad \text{for } 1 < \gamma < 4 \quad (2)$$

$$B = \frac{5}{4} f_o^4 \quad (3)$$

$$\alpha = e^{-\frac{(f-f_o)^2}{2\sigma^2 f_o^2}} \quad (4)$$

$$\sigma = 0.07 \quad \text{for } f \leq f_o$$

$$\sigma = 0.09 \quad \text{for } f > f_o$$

$f_o$  is the peak frequency(Hz);  $H_s$  is the significant wave height ( $m$ ), and  $\gamma$  is the peak enhancement factor. A value of 3.3 was assigned to the variable  $\gamma$  in all wave tank experiments.

## 6. The neural network

An artificial neural network (ANN) is a mathematical model that tries to imitate the structure and functionality of a biological neural network. It has the ability to model complex nonlinear problems with practically accepted accuracy. The experimental data are used to train the neural network; more details are mentioned in the following section. In general, it consists of an input layer, one or more hidden layers and an output layer. A bias can be added to the input layer and each hidden layer. The design of the network structure is based on its function. For the problem at hand, a feed-forward back-propagation network with an input layer, one hidden layer having 50 neurons and an output layer was enough to simulate the problem accurately. A MATLAB neural tool box is used to design and train a neural network to use deck acceleration measurements to predict the bending moment acting at the base of the model. Fig. 5 depicts the neural network used in the analysis.

Several neural networks having different hidden layer structure, number of neurons and training functions were tried. No significant improvement was obtained by adding more than one hidden layer to the network. The Levenberg-Marquardt back propagation training technique was used to train the network. A hyperbolic tangent sigmoid transfer function and a linear transfer function were used for the hidden and output layers, respectively. The performance of the network is measured using the mean square error (MSE). The data was randomly divided into three sets: 60% for training, 20% for validation, and 20% for testing. Fig. 6 shows the change in the MSE with the epochs during the training process. It should be noted that the input and target data were not normalized. Fig. 7 shows the regression of the training, validation, and testing sets, respectively during the training process. Once the network is trained, it is applied to the whole data and the regression of the input and the output is shown in Fig. 8. Comparison between the moment's

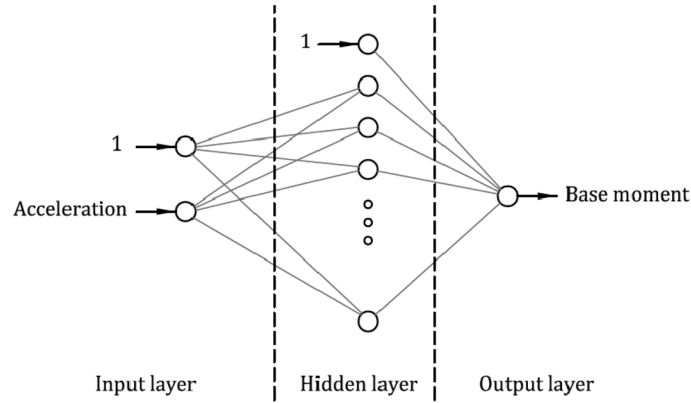


Fig. 5 Neural network structure

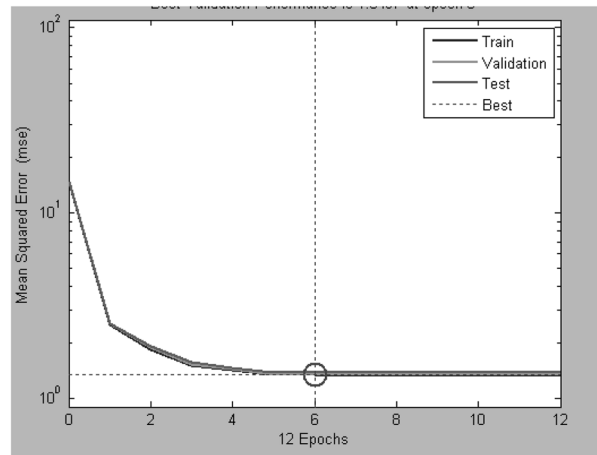


Fig. 6 Mean square error against epochs during training

measured and simulated time histories is shown in Fig. 9. Comparison between the measured and neural network standard deviations is given in Table 1. Fig. 10 shows a comparison of the measured and predicted autocorrelation functions of the bending moment at base. Fig. 11 shows a comparison of the FFT for the measured and predicted bending moments. The standard deviation, autocorrelation function and the FFT provide suitable tools to compare random process data. The predictions obtained by the neural network are highly accurate and the computer time needed for the analysis is short.

## 7. Experimental estimation of the reaction force and bending moment at base

The model was instrumented with a number of strain gages located on the fore and aft sides of the model. The distance between two consecutive sensors is approximately 17 cm. The notation for shear and moment at base is shown in Fig. 12. The bending moment can be calculated to be

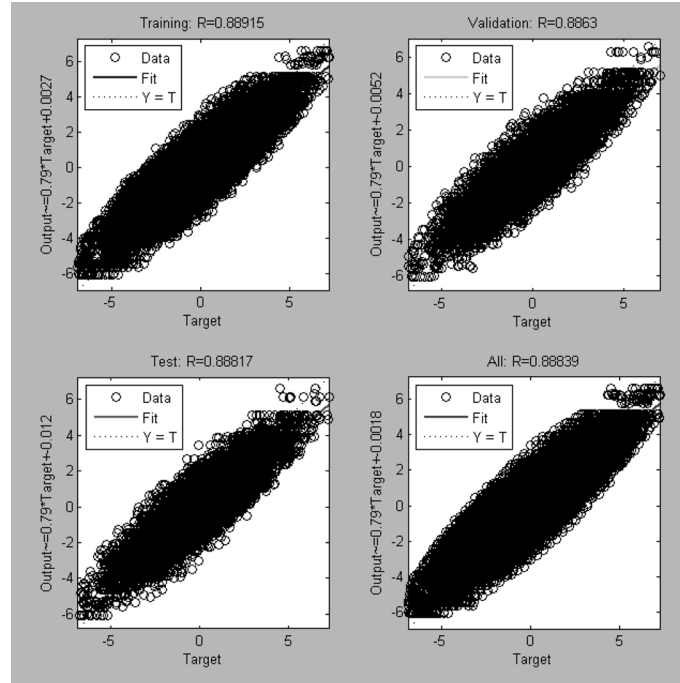


Fig. 7 Regression of training, validation and testing sets

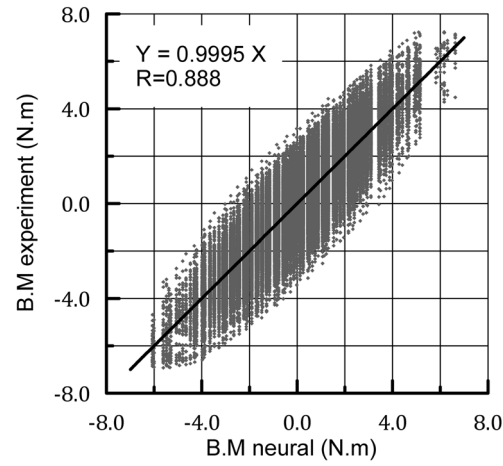


Fig. 8 Regression of the whole data

$$M = \frac{\pi E \varepsilon (D_o^4 - D_i^4)}{32 D_o} \quad (5)$$

where  $M$  is the bending moment,  $E$  is the modulus of elasticity,  $\varepsilon$  is the strain tension or compression strain at extreme fibre,  $D_o$  is the outer diameter,  $D_i$  is the internal diameter of the tube. The value of the strain used is the average of the strains at extreme fibers of the tube. This means the elimination of the strains due to compressive forces on the tube section.

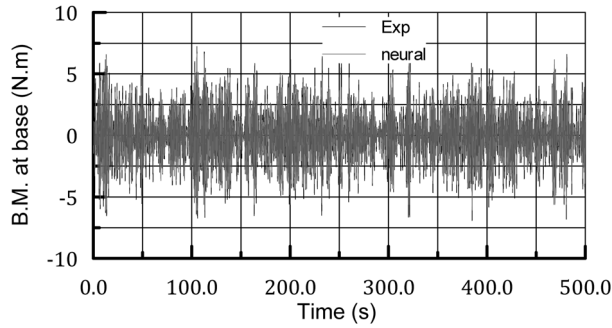


Fig. 9 Moment time history

Table 1 Comparison between experiment and neural network output

item	Standard deviation, $\sigma$ of measured reaction (N)	Standard deviation, $\sigma$ of B.M at base (N. m)
Experiment	0.866	2.28
Neural networks	0.722	2.03
difference	16.62 %	10.96 %

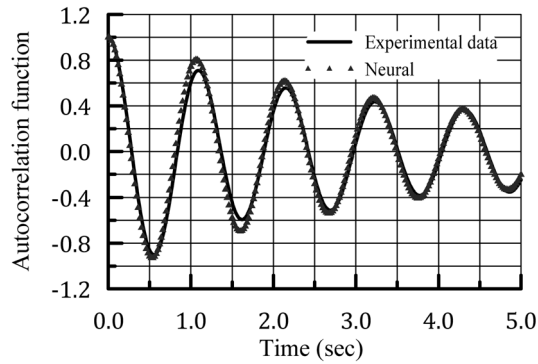


Fig. 10 Moment auto-correlation

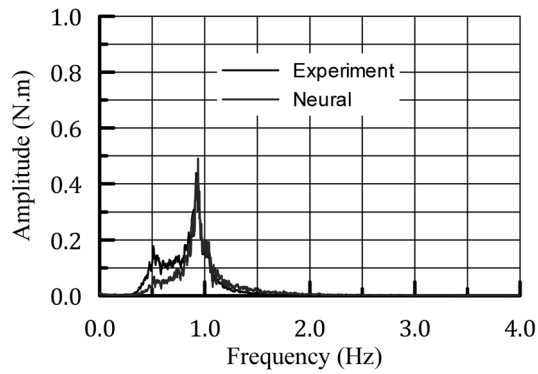


Fig. 11 Moment FFT

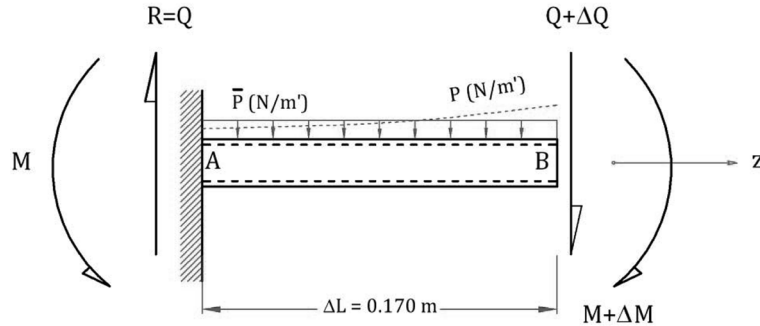


Fig. 12 Calculation of reaction force at base

To calculate the reaction force at the base, the following procedure is followed. Approximating the variable water pressure  $P$  on a small distance by a constant value  $\bar{P}$  and taking the moment around point B, the following equation is derived

$$(M + \Delta M) - M + R \times \Delta L - \bar{P} \times (\Delta L)^2 / 2 = 0 \quad (6)$$

The reaction force can be calculated as

$$R = -5.88\Delta M + 0.085\bar{P} \quad (7)$$

The second term in the right hand side of eq. (7) can be neglected since the wave pressure near the sea bed is very small.

Based on eq. (7) and using two measuring points (4 strain gages), the time history of the reaction at the base can be estimated. A neural network is used to estimate the reaction force at base as a function of the top acceleration. Fig. 13 shows the mean square error during the training process for the shear at base estimation. It should be noted that the actual values for the acceleration at the

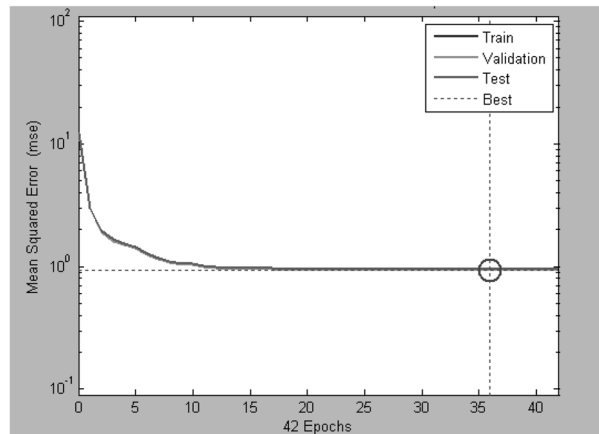


Fig. 13 Mean square error against epochs

model's top were used as input to the moment and force networks. No normalization for the input was attempted. Fig. 14 shows a comparison between the measured and network time histories for the reaction force. The neural network was able to estimate the reaction force at base with sufficient accuracy. In spite of the high number of input data ( $\approx 50000$  data points), the neural network was able to converge in a very short time. Fig. 15 shows the relationship between the measured and

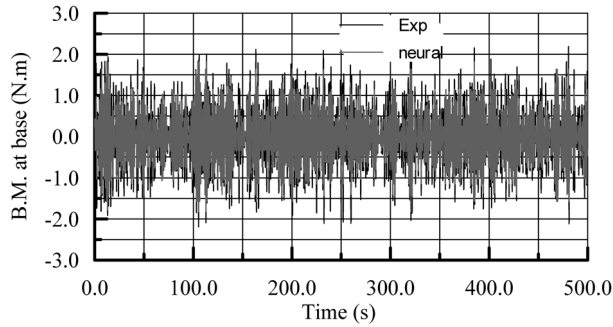


Fig. 14 Time history comparison of reaction force at base

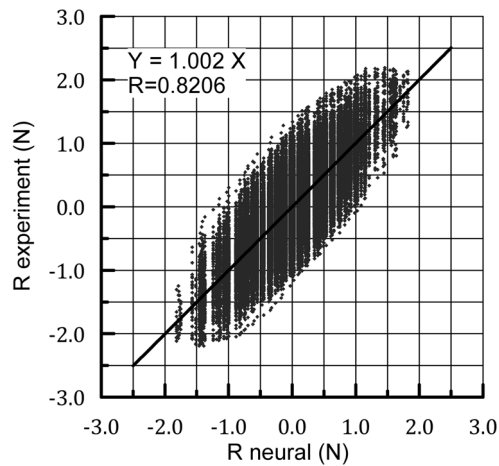


Fig. 15 Reaction at base comparison

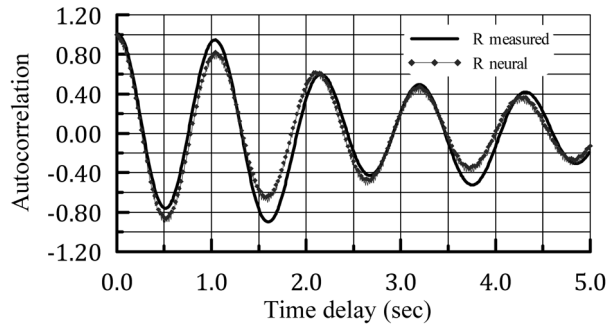


Fig. 16 Autocorrelation comparison of R at base

predicted values for the reaction force. Fig. 16 shows a comparison between the autocorrelation function of the measured and predicted reaction force.

## 8. Experimental estimation of the excitation

Approximating the system by a single degree of freedom system, the equation of motion can be written as

$$m\ddot{x}(t) + c\dot{x}(t) + kx(t) = F(t) \quad (8)$$

$m$  stands for total virtual mass,  $c$  for damping,  $k$  for stiffness,  $t$  for time and  $F(t)$  for the external force. The total virtual mass is the sum the physical mass and the hydrodynamic added mass. Eq. (8) can be normalized with respect to the total mass,  $m$  to be

$$\ddot{x}(t) + \frac{c}{m}\dot{x}(t) + \frac{k}{m}x(t) = \frac{F(t)}{m}$$

or

$$\ddot{x}(t) + 2\xi\omega_o\dot{x}(t) + \omega_o^2x(t) = f(t) \quad (9)$$

$\omega_o$  is the natural frequency of the system (rad/s),  $\xi$  is the damping ratio,  $f(t)$  is the force per unit total virtual mass,  $x(t)$  is the response at time  $t$  of the system. A dot over the variable means differentiation w.r.t. the time.

The random excitation  $f(t)$  is assumed to satisfy the following condition

$$\begin{aligned} \langle f(t) \rangle &= 0 \\ \langle f(t) \rangle f(t + \tau) &= \psi_o \delta(\tau) \end{aligned} \quad (10)$$

$\delta$  is the Dirac delta and  $\psi_o$  is the variance of the excitation. The following change of variables is used

$$y_1 = x, \quad y_2 = \dot{x} \quad (11)$$

Using the change of variables (11) in eq. (9), one gets

$$\begin{aligned} \dot{y}_1 &= y_2 \\ \dot{y}_2 &= -2\omega_o\xi y_2 - \omega_o^2 y_1 + f(t) \end{aligned} \quad (12)$$

Haddara (2006) showed that the conditional probability density function  $P(Y, t | Y_o)$  governing the random process  $Y(t) = \begin{Bmatrix} y_1 \\ y_2 \end{Bmatrix}$  satisfies the Fokker-Plank equation given by

$$\frac{\partial P}{\partial t} = -\frac{\partial}{\partial y_1}(y_2 P) + \frac{\partial}{\partial y_2}(y_1 \{2\xi\omega_o y_2 + \omega_o^2 y_1\} P) + \frac{\psi_o \partial^2 P}{2 \partial y_2^2} \quad (13)$$

Multiplying Eq. (13) by  $y_1^2$ ,  $y_2^2$  and  $y_1 y_2$  respectively, then integrating the equation over the complete domain of the variables  $y_1, y_2$  and  $y_{12}$ , the following equations can be derived

$$\begin{aligned} \dot{v}_{11} &= 2 v_{12} \\ \dot{v}_{22} &= -2 \langle 2\xi\omega_o y_2^2 + \omega_o^2 y_1 y_2 \rangle + \psi_o \\ \dot{v}_{12} &= v_{22} - \langle 2\xi\omega_o y_1 y_2 + \omega_o^2 y_1^2 \rangle \end{aligned} \quad (14)$$

$v_{11}$  is the variance of the displacement,  $v_{22}$  is the variance of the velocity, and  $v_{12}$  is the covariance of displacement and velocity.

Since the random variables are stationary, the derivatives on the left hand side of equation (14) are zeros, thus

$$\begin{aligned} v_{12} &= 0 \\ \psi_o &= 4\xi\omega_o v_{22} \\ v_{22} &= \omega_o^2 v_{11} \end{aligned} \quad (15)$$

The variance of the acceleration  $v_{33}$  can be derived as

$$v_{33} = \langle \ddot{y}_2^2 \rangle = \omega_o^2 v_{22} \quad (16)$$

Combining eqs. (15) and (16)

$$\psi_o = \frac{4\xi v_{33}}{\omega_o} \quad (17)$$

Because the response of the platform is random in case of random excitation, it is important to relate the variance of the excitation to the range of the acceleration at the deck of the structure. Eq. (17) relates the variance of the normalized external excitation to the variance of the acceleration. The FFT (Fast Fourier Transform) of the acceleration in case of no added deck masses is shown in Fig. 17 which gives the approximate value of the natural frequency. Applying the random decrement technique (RD) to the acceleration time history, the free decay shown in Fig. 18 is extracted.

## 9. Effect of changing the concentrated mass at the free end

The relation between the normalized exciting force in eq. (9) and the actual force in eq. (8) is the total virtual mass,  $m$ . This section discusses how to estimate this total virtual mass at different deck masses. The deck's mass was varied by attaching a concentrated mass to the deck. Several tests

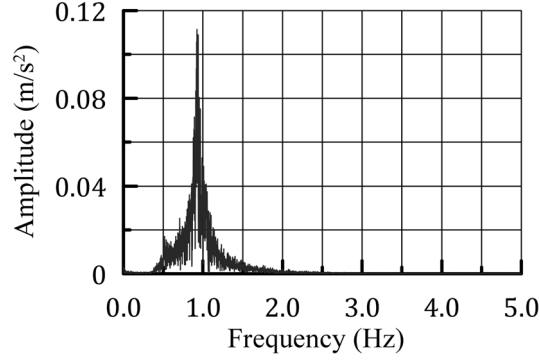


Fig. 17 FFT of the acceleration time history

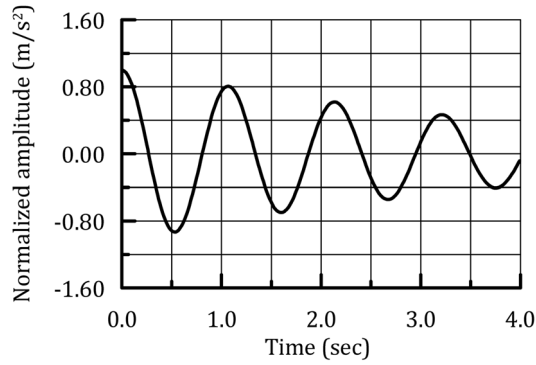


Fig. 18 RD of the acceleration

were done using different values for the mass on deck. The analysis for the data and the results obtained are reported in this section.

The damped natural frequency can be obtained from the time of one cycle of the random decrement graph given in Fig. 18. The logarithmic decrement  $\delta$  can be calculated using eq. (17).

$$\delta = \frac{1}{n} \ln \left( \frac{A_i}{A_{i+n}} \right) \quad (18)$$

where  $A_i$  are  $A_{i+n}$  the amplitudes of the and  $(i+n)$ th cycles, respectively.

The modal damping,  $\xi$  is related to the logarithmic decrement  $\delta$  by the equation

$$\xi = \frac{\delta}{\sqrt{4\pi^2 + \delta^2}} \quad (19)$$

The undamped natural frequency can be calculated from the equation

$$\omega_o = \frac{\omega_d}{\sqrt{1 - \xi^2}} \quad (20)$$

Table 2 Effect of the Deck's concentrated mass

Deck's mass (kg)	Damping ratio, $\xi$	Undamped natural freq. $\omega_o$ , (rad /sec)	Norm. var., $\psi_o$	Total virtual mass, $m$ (kg)
0.000	0.0400	5.8762	0.00390	12.06
0.454	0.0357	5.5313	0.00426	12.97
1.000	0.0376	5.1119	0.00504	12.79
2.000	0.0536	4.5817	0.00651	11.32
2.500	0.0542	4.3595	0.00701	11.24

The variance of the measured acceleration is obtained from its recorded time history. Using eq. (16), the variance of the normalized excitation ( $f$ ) can be obtained. The reaction force  $R$  at the base of the model is considered to be equal to the wave exciting force  $F$  acting on the equivalent single degree of freedom system. The variance of the reaction force can be obtained from the strain gages measurement as explained above. One can then estimate the total virtual mass,  $m$  of the equivalent single degree of freedom system of the model using the following equation:

$$m = \frac{\sqrt{\text{var}(F(t))}}{\sqrt{\text{var}(f(t))}} \quad (21)$$

Table 2 shows the results obtained when the concentrated mass at the free end of the model was changed.

## 10. Conclusions

This paper reports the results of an experimental program which aims at finding a relationship between the measured deck mass of a single column platform to the health condition of the foundation of the platform. The long range objective is to extrapolate this study to other forms of offshore platforms. Using artificial neural networks we were able to find a fairly accurate relationship between the measured acceleration and the moment at the foundation. The moment at the foundation was determined from the readings of strain gages placed near the foundation. The reaction force at the foundation was obtained from the bending moment acting on the platform at two sections 17 apart. Several measures were used to test the quality of the neural network estimate in both the reaction force and bending moment at base. Among of these measures are the regression between the estimated and measured data, time history comparisons, autocorrelation functions comparisons, the smoothed spectrums, and the values of the standard deviations.

The Fokker-Planck equation was also used to relate the variance of normalized external excitation to the variance of the measured acceleration. The random decrement of the acceleration was calculated and used to estimate the damping and natural frequency of the structure. The acceleration measurements are related to the reaction at the foundation using an equivalent single degree of freedom formulation; all the parameters used in the equation were successfully estimated. The total virtual mass for the equivalent SDOF system was calculated at different added deck masses. Table 2 showed that the estimated total virtual mass for the equivalent system varied between 11.24 and 12.97 Kg. This represents about 13.3% variation in the value of the total virtual mass for the

equivalent system. The estimated virtual mass relates the normalized exciting force to the actual force. This approach does not require a large computer time to perform the analysis. This makes it a reasonable candidate for an online foundation health monitoring system.

## Acknowledgements

The authors would like to thank PRAC, MITACS, and NSERC for financial support and Memorial University for providing test facility.

## References

- Arena, F. and Puca, S. (2004), "The Reconstruction of Significant Wave Height Time Series by Using a Neural Network Approach", *J. Offshore Mech. Arct.*, **126**(3), 213-219.
- Banerji, P. and Datta, T.K. (1997), "Integrity monitoring of offshore platforms using artificial neural nets", *Proceedings of the 1997 7th International Offshore and Polar Engineering Conference*, Honolulu, USA, May.
- Budipriyanto, A., Haddara, M. and Swamidas, A. (2007), "Identification of damage on ship's cross stiffened plate panels using vibration response", *Ocean Eng.*, **34**(5-6), 709-716.
- Chang, S., Kim, D., Chang, C. and Cho, S.G. (2009), "Active response control of an offshore structure under wave loads using a modified probabilistic neural network", *J. Mar. Sci. Technol.*, **14**(2), 240-247.
- Diao, Y., Li, H., Shi, X. and Wang, S. (2005), "Damage localization for offshore platform by neural networks", *Proceedings of the International Conference on Machine Learning and Cybernetics*, Guangzhou, China, August.
- Elshafey, A.A., Haddara, M.R. and Marzouk, H. (2009), "Identification of the excitation and reaction forces on offshore platforms using the random decrement technique", *Ocean Eng.*, **36**(6-7), 521-528.
- Elshafey, A.A., Haddara, M.R. and Marzouk, H. (2010), "Identification of excitation and reaction forces spectra for offshore platforms", *Can. J. Civ. Eng.*, **37**(1), 66-76.
- Elshafey, A.A., Haddara, M.R. and Marzouk, H. (2010), "Damage detection in offshore structures using neural networks", *Mar. Struct.*, **23**(1), 131-145.
- Fathi, A. and Aghakouchak, A.A. (2007), "Prediction of fatigue crack growth rate in welded tubular joints using neural network", *Int. J. Fatigue*, **29**(2), 261-275.
- Haddara, M.R. (2006), "Complete Identification of the Roll Equation using the Stationary Random Roll Response", *J. Ship Res.*, **50**(4), 388-397.
- Londhe, S. and Panchang, V. (2005), "One-Day Wave Forecasts Using Buoy Data and Artificial Neural Networks", *Proceedings of the MTS/IEEE OCEANS*, Washington, DC, USA, September.
- Lopes, T.A.P. (1997), "Neural networks on fatigue damage prediction", *Proceedings of the 1997 IEEE International Conference on Neural Networks*, Houston, USA, June.
- Lopes, T.A.P. and Ebecken, N.F.F. (1997), "In-time fatigue monitoring using neural networks", *Mar. Struct.*, **10**(5), 363-387.
- Ma, R., Li, G., Zhao, D., and Wang, J. (2007), "Experimental study of wave forces on vertical cylinders in shallow waters". *Proceedings of the 26th International Conference on Offshore Mechanics and Arctic Engineering*, San Diego, California, USA, June.
- Rahman, M.S., Wang, J., Deng, W. and Carter, J.P. (2001), "A neural network model for the uplift capacity of suction caissons", *Comput. Geotech.*, **28**(4), 269-287.
- Simões, M.G., Tiquilloca, J.L.M. and Morishita, H.M. (2002), "Neural-network-based prediction of mooring forces in floating production storage and offloading systems", *IEEE T. Ind. Appl.*, **38**(2), 457-466.
- Yun, C. and Bahng, E.U. (1997), "Substructural identification of offshore structures using neural networks", *Proceedings of the International Offshore and Polar Engineering Conference*, Honolulu, USA, May.
- Zubaydi, A., Haddara, M.R. and Swamidas, A.S.J. (2002), "Damage Identification in a Ship's Structure Using Neural Networks", *Ocean Eng.*, **29**(10), 1187-1200.